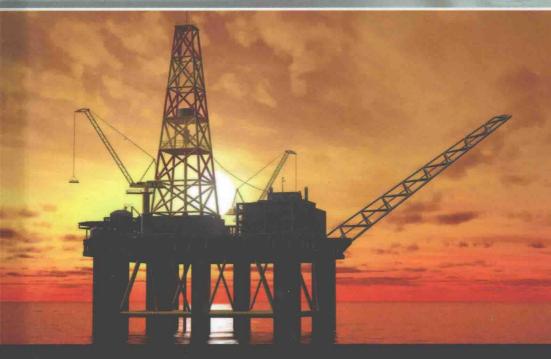


ELSEVIER INSIGHTS



TURBULENCE IN POROUS MEDIA

MODELING AND APPLICATIONS

SECOND EDITION

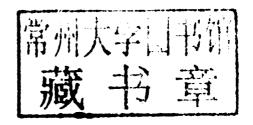
MARCELO J. S. DE LEMOS

Turbulence in Porous Media Modeling and Applications

Second Edition

Marcelo J.S. de Lemos

Instituto Tecnológico de Aeronáutica—ITA, Brazil





Elsevier

32 Jamestown Road, London NW1 7BY 225 Wyman Street, Waltham, MA 02451, USA

First edition 2006 Second edition 2012

Copyright © 2012 Elsevier Ltd. All rights reserved

No part of this publication may be reproduced or transmitted in any form or by any means, electronic or mechanical, including photocopying, recording, or any information storage and retrieval system, without permission in writing from the publisher. Details on how to seek permission, further information about the Publisher's permissions policies and our arrangement with organizations such as the Copyright Clearance Center and the Copyright Licensing Agency, can be found at our website: www.elsevier.com/permissions

This book and the individual contributions contained in it are protected under copyright by the Publisher (other than as may be noted herein).

Notices

Knowledge and best practice in this field are constantly changing. As new research and experience broaden our understanding, changes in research methods, professional practices, or medical treatment may become necessary.

Practitioners and researchers must always rely on their own experience and knowledge in evaluating and using any information, methods, compounds, or experiments described herein. In using such information or methods they should be mindful of their own safety and the safety of others, including parties for whom they have a professional responsibility.

To the fullest extent of the law, neither the Publisher nor the authors, contributors, or editors, assume any liability for any injury and/or damage to persons or property as a matter of products liability, negligence or otherwise, or from any use or operation of any methods, products, instructions, or ideas contained in the material herein.

British Library Cataloguing-in-Publication Data

A catalogue record for this book is available from the British Library

Library of Congress Cataloging-in-Publication Data

A catalog record for this book is available from the Library of Congress

ISBN: 978-0-08-098241-0

For information on all Elsevier publications visit our website at store elsevier com

This book has been manufactured using Print On Demand technology. Each copy is produced to order and is limited to black ink. The online version of this book will show colour figures where appropriate.

Working together to grow libraries in developing countries

www.elsevier.com | www.bookaid.org | www.sabre.org

ELSEVIER

BOOK AID International

Sabre Foundation

Turbulence in Porous Media

to the memory of Floriano Eduardo de Lemos to Magaly, Pedro and Isabela

Preface to the First Edition

The main idea of this monograph is to introduce the reader to the possible characterizations of turbulent flow, and heat and mass transport in permeable media, including analytical, numerical and a review of available experimental data. Such transport processes, occurring at relatively high velocity in permeable media, are present in a number of engineering and natural flows. Therefore, a book like this one that compiles, details, compares and evaluates the available methodologies in the literature for modeling and simulating such flows can be useful to different fields of knowledge, covering engineering (mechanical, chemical, aerospace and petroleum) and basic sciences (thermal sciences, chemistry, physics, applied mathematics, and geological and environmental sciences).

This work has as its primary audience graduated students, engineers and scientists involved in design and analyses of: (a) modern engineering system such as fuel cells, porous combustors and advanced heat exchangers, (b) studies of biomechanical problems such as air flow in lungs and (c) modeling of natural and environmental flows such as atmospheric boundary layer over vegetation, fire in forests and spread of contaminants near rivers and bays.

In regard to already published works, it looks to the author that a book on the specific topic of "turbulence in porous media" is still not yet available as this topic is still quite new and unexplored. Only a few years ago papers on this topic have started to appear in scientific journals.

This book was written for use in graduate courses on turbulent transport phenomena in engineering, chemical and environmental programs which deal with research areas involving this theme.

My former and present graduate students have all contributed to the completion of this monograph. In the book, I also tried to collect, review and compile some of our joint publications and reports, which were completed during the last fifteen years or so. My sincere thanks to all of them, which includes Drs Pedras, M.H.J., Rocamora Jr., F.D., Assato, M., Braga, E.J., Mesquita, M.S., doctoral candidates Silva, R.A., Saito, M.B., Tofaneli, L.A., master graduates Magro, V.T., Graminho, D.R. and Santos, N.B.

Our research sponsors, CNPq and FAPESP (Brazilian Federal and São Paulo State Research Funding Agencies, respectively) have also greatly contributed to our "existence" as a research group. Most of my graduate students so far have been funded by them. To CNPq and FAPESP, my sincere thanks and my hopes that they keep on believing in our work.

In my nearly twenty years of teaching at Instituto Tecnológico de Aeronáutica (ITA), Brazil, I have always had support from colleagues and the Institute

administration. None of our research goals would have been accomplished if we had been exposed to an "adverse pressure gradient" during these years. ITA, consistently and continually, has provided a fruitful and open environment were new ideas find fertile ground to grow and develop. I wish to express my sincere thanks to ITA and all the colleagues of the Mechanical Engineering Division.

A prominent professor in Brazil recently said that in the post-war era the international language spoken in most meetings and conferences around the world is "Bad English". Transposing this notion to written material, I wish to convey my deep apologies to all native English speakers for doing so much damage to Shakespeare's language.

The idea of writing this book came from a conversation I had with the senior publishing editor of Elsevier Arno Schouwenburg, who trusted that I had adequate scholarship for putting forward this project. I am grateful to him and to Vicki Wetherell, Editorial Assistant, for their invaluable help during the preparation of this work.

Finally, I hope that this work does not disappoint the reader who wishes to keep abreast with the latest developments in the interesting and innovative field of modeling turbulence in permeable structures.

Marcelo J.S. de Lemos São José dos Campos, September 2005



This photo, with my father¹ and son, is to me unmistakable evidence that, in our short life, uncertainty and fear lie in between youth hopefulness and old age wisdom.

¹ During the production stage of the first edition of this book, Prof. Dr. Floriano Eduardo de Lemos passed away.

Preface to the Second Edition

Five years after publication of the first edition of this book it is about time to revise and expand the information presented in this text. During this period, several groups around the world started working on double-averaging techniques and we, at ITA, were led to believe that somehow the book played a role in the dissemination of new ideas and in the overwhelming response that those thoughts have had within the community. Not a single month has passed without a paper on such theme to be reviewed by us. On the overall, authors have worked on similar treatments for turbulence in porous media and at several levels of complexity, sometimes combining what was already understood and detailed, some other instances dividing the turbulence spectrum into bands, each of which handled by its own transport equation. In most works, however, the time-volume or volume-time sequence of integration has played always a role in setting up the overall modeling strategy.

We, at ITA, have also worked on some additional progress in extending the original model to situations including reactive systems, where an exothermic reaction rate in the porous material was allowed to take place in the space occupied by a flowing gaseous phase. This additional development is documented in Chapter 8. Combustion in inert porous materials could then be tackled and important technological applications, such as porous burners, hydrogen production systems and fuel cells, can now benefit from the ideas first described in the original book. Governing equations were rewritten allowing for burning rates in the fluid phase and, in the iterative cycle for numerical solution of the equations, density updates were considered as temperature increases due to release of heat.

Other important development discussed in this second edition is that concerned with the movement of the porous matrix. In a number of engineering flows of practical relevance, as in gasification processes and in manufacturing of advanced materials, one can identify a permeable bed that is moving, either parallel to the working fluid or in the oppose direction to it. Transport equations were then extended to account for the motion of the porous bed and both fields analyzed, the time-volume-averaged and the statistical one, had their governing equations modified in order to cope with the movement of the solid matrix. Chapter 9 documents this development.

My former graduate students R.A. Silva, M.B. Saito and L.A. Tofaneli, doctoral candidates at the time when the first edition came out, have all concluded their Doctoral research programs. I am thankful to them for contributing to our overall goal of developing a tool with an ever-wider range of application. My former Master students C. Fischer and F.T. Dórea have also made an excellent job in

applying and testing the developed model. Currently, doctoral candidate A.C. Pivem is working hard at evaluating the treatment of moving beds and their application to practical situations. Master student J.E.A. Coutinho is also helping to evaluate the combustion model in porous burners. To all my former and current students, my sincere thanks and appreciation for their dedication and hard work.

As in the first edition of the book, I would like to cite the names of our research funding agencies in Brazil, FAPESP and CNPq, for their continuous support. One additional agency that unfortunately was missing in the first edition is CAPES, which is directly under the Ministry for Education and Culture (MEC) in Brazil. To all three of them, CAPES, FAPESP and CNPq, my sincere thanks and my hopes for a continuous support on our work in the years to come.

The writing of this second edition was motivated by the very many e-mails and personal communications in meetings and conferences during the last five years since the introduction of the book. Apparently, colleagues worldwide have praised our work and the many review requests mentioned above indicated to us that, somehow, the book has had a positive impact in the literature. A second edition was then due in order to expand the earlier ideas and to further exploit the theme. Then, after deciding to write this second edition, I contacted Elsevier and learned that sales figures of the printed book did not justify a second printed edition. Surprised by this outcome, I have done some research on what could be the reason for such apparent contradiction. Or say, even though the book had, to a certain extent, motivated new research by others in addition to provoking a number of revision requests, e-mails and a couple of (fully covered) keynote lectures in conferences and meetings, the truth of the matter was that the first edition was, at the end, a financial disaster to the publisher! With the help of a student and after "surfing" for some time on the Internet, I realized the existence of many unauthorized websites from where the book could be freely downloaded. Needless to say, the same happens nowadays with whatever material that can be made digital. My conclusion was that, if for one side profits where not attractive enough to justify a second edition, the overwhelming response that the book seems to have had from the community was unquestionable, even though (or perhaps because) the digital material was made available for free to many. Finally, I wish to express my gratitude to Mrs. Stefani Montemagni for her careful and skilful typing of the manuscript.

> Marcelo J.S. de Lemos São José dos Campos, December 2011

Overview

The main focus of this book is to present, in an organized, self-contained, and systematic format, new engineering techniques and novel applications of turbulent transport modeling for flow, heat, and mass transfer in porous media. The motivation for writing this text is the fact that modern engineering equipment design and environmental impact analyses can benefit from the appropriate modeling of turbulent flow in permeable structures. Examples span from flow in advanced porous combustors to atmospheric boundary layers over thick and dense rain forests. This is a very new topic because it involves disciplines that, traditionally, have been developed separately, such as *turbulence*, mostly associated with clear (unobstructed) flows, and *porous media*, which is usually related to low-speed currents, in the laminar regime, through beds or materials containing interconnected pores.

Accordingly, a number of natural and engineering systems can be characterized by some kind of porous structure through which a working fluid permeates in the turbulent regime. That is the case of many transport systems in environmental, petroleum, chemical, mechanical, and aerospace technologies, including flows and fires in rain forests, for example. Here, forests are modeled as porous layers through which atmospheric air flows. In fact, forest fires devastate huge amounts of land and occur frequently in many countries such as Canada and Brazil. The ability to predict the spread of fire fronts more precisely, for example, might help authorities to better manage resources to minimize risk to human life. For analyzing such systems in a realistic and useful way, one has to consider the heterogeneity of the medium (different phases) and the fact that the flow fluctuates with time.

Another important application is the analysis of flow and heat transfer in advanced energy systems such as fuel cells and porous combustors. In addition, many transport processes in chemical engineering equipment also occur at a high velocity within a porous bed. The two independent characteristics mentioned previously (namely, the medium heterogeneity and flow turbulence) have never been covered in a book and, as mentioned, this new knowledge could be useful to scientists, engineers, and environmentalists dealing with natural disasters and working on the development of advanced energy systems.

As such, for practical, simple, and tractable analyses, engineers, scientists, and environmentalists tend to look at these systems as if the medium were made by a unique material (after application of a volumetric average) and did not present high-frequency variation in its fluid-phase velocity (by using a model for handling turbulence effects). The advantages of having an easy-to-use tool based on this macroscopic treatment are many, such as unveiling important overall flow

xviii Overview

characteristics without having to resort to sole experimental analysis, which, in turn, can be time consuming and expensive.

Turbulence models proposed for such flows depend on the order of application of time- and volume-averaged operators. Two developed methodologies, following the two orders of integration, lead to different governing equations for the statistical quantities. This book will review recently published methodologies to characterize turbulent transport in porous media mathematically.

The concept of *double decomposition* is discussed in detail, and models are classified in terms of the order of application of time- and volume-averaged operators, among other peculiarities. A total of four major classes of models have been identified, and a general discussion on their main characteristics takes place.

For hybrid media, involving both a porous structure and a clear flow region, difficulties arise due to the proper mathematical treatment given at the interface. This book also presents and discusses numerical solutions for such hybrid media, considering a channel partially filled with a porous layer through which fluid flows in the turbulent regime. In addition, macroscopic forms of buoyancy terms were considered in both the mean and the turbulent fields. Cases reviewed include heat transfer in porous square enclosures, as well as cavities partially and totally filled with porous material.

In summary, this book presents an overview of both porous media modeling and turbulence modeling, with the aim of positioning this work in relation to these two classical analyses. It begins with a review of governing equations for clear flow before the averaging operations are applied to them. Then the double-decomposition concept is presented and thoroughly discussed prior to the derivation of macroscopic governing equations. Equations for turbulent momentum transport follow, showing detailed derivation for the mean and turbulent field quantities. The statistical $k-\varepsilon$ model for clear domains, used to model turbulence effects, also serves as the basis for modeling. Turbulent heat transport in porous matrices is then reviewed in light of the double-decomposition concept. Models for treating buoyancy effects, double diffusion, reactive flows, and systems having a moving solid phase are also considered in the book. A chapter on numerical modeling and algorithms details major methodologies and techniques used to solve the flow governing equations numerically. A final chapter on applications in hybrid media covers forced flows in composite channels, channels with porous and solid baffles, turbulent impinging jet onto a porous layer, buoyant flows, heat transfer in a back-step and heat transport in porous burners and in moving beds.

List of Figures

Figure 1.1	Examples of an EOR system.	7
Figure 1.2	The influence of the Reynolds number of a fine	
	turbulence structure: (A) Low Reynolds number,	
	(B) High Reynolds number.	11
Figure 1.3	Flow regimes over permeable structures.	16
Figure 1.4	A macroscopic analysis of heat exchangers.	17
Figure 1.5	A macroscopic view of flow over rain forests.	17
Figure 2.1	Representative Elementary Volume (REV) showing intrinsic	
C	and time averages as well as deviation and time fluctuation of	
	a general variable φ .	
	Source: From Pedras and de Lemos (2001a), with	
	permission.	22
Figure 2.2	Time averaging over length of time Δt .	24
Figure 3.1	A general three-dimensional vector diagram for a quantity	
	φ (see Rocamora and de Lemos, 2000a).	30
Figure 4.1	A model of REV—periodic cell and elliptically generated	
	grids: (A) longitudinal elliptic rods, $a/b = 5/3$ (Pedras and	
	de Lemos, 2001c); (B) cylindrical rods, $a/b = 1$ (Pedras and de	
	Lemos, 2001a); and (C) transverse elliptic rods, $a/b = 3/5$	
	(Pedras and de Lemos, 2003).	46
Figure 4.2	Microscopic results at $Re_H = 1.67 \times 10^5$ and $\phi = 0.70$ for	
	longitudinal ellipses: (A) velocity; (B) pressure; (C) k;	
	and (D) ε .	48
Figure 4.3	Microscopic results at $Re_H = 1.67 \times 10^5$ and $\phi = 0.70$	
	for transversal ellipses: (A) velocity; (B) pressure; (C) k;	
	and (D) ε .	49
Figure 4.4	Overall pressure drop as a function of Re_H	
	and medium morphology.	50
Figure 4.5	The effect of porosity and medium morphology on the	
	overall level of turbulent kinetic energy.	51
Figure 4.6	Macroscopic turbulent kinetic energy as a function	
	of medium morphology and Re_H .	52
Figure 4.7	Numerically obtained permeability $K(m^2)$ as a function	
	of medium morphology.	52
Figure 4.8	Determination of the value of c_k using data for	
	different medium morphology.	53
Figure 5.1	Unit cell and boundary conditions: (A) macroscopic velocity	
	and temperature gradients; given temperature difference	
	at the east-west boundaries; (B) longitudinal gradient,	
	Eq. (5.52); (C) transversal gradient, Eq. (5.53); given heat	

xx List of Figures

	fluxes at the north-south boundaries; (D) longitudinal	
	gradient; (E) transversal gradient.	62
Figure 5.2	A temperature field with imposed longitudinal temperature	
	gradient, $\phi = 0.60$. Given temperature difference at the	
	east-west boundary (see Eq. (5.52))—(A) $Pe_H = 10$; (B)	
	$Pe_H = 4 \times 10^3$; given heat fluxes at the north-south boundary	
	(see Figure 4.1D)—(C) $Pe_H = 10$; (D) $Pe_H = 4 \times 10^3$.	66
Figure 5.3	A temperature field with imposed transversal temperature	
	gradient, $\phi = 0.60$. Given temperature difference at the	
	north-south boundary (see Eq. (5.53))—(A) $Pe_H = 10$; (B)	
	$Pe_H = 4 \times 10^3$; given heat fluxes at the north-south boundary	
	(see Figure 4.1E)—(C) $Pe_H = 10$; (D) $Pe_H = 4 \times 10^3$.	67
Figure 5.4	Longitudinal thermal dispersion: (A) $\phi = 0.60$ and	07
riguic 5. i	(B) overall results.	68
Figure 5.5	Longitudinal thermal dispersion comparing $k_s/k_f = 2$	00
riguic 3.3	and $k_s/k_f = 10$. (A) Neumann boundary conditions	
	(Figure 5.1D); (B) temperature boundary conditions	
	(Figure 5.1B, Eq. (5.52)).	70
Figure 5.6	Transverse thermal dispersion: (A) $\phi = 0.60$	70
riguic 5.0	and (B) overall results.	71
Figure 5.7	Transverse thermal dispersion comparing $k_s/k_f = 2$ and	/ 1
riguic 3.7	$k_{s}/k_{f} = 10$. (A) Neumann boundary conditions (Figure 5.1E);	
	(B) temperature boundary conditions (Figure 5.1C, Eq. (5.53)).	72
Figure 5.8	A physical model and coordinate system.	75
Figure 5.9	A nonuniform computational grid.	76
Figure 5.10	A velocity field for $Pr = 1$ and $Re_D = 100$.	77
Figure 5.11	Isotherms for $Pr = 1$ and $Re_D = 100$.	77
Figure 5.11	The effect of Re_D on h_i for $Pr = 1$; solid symbols denote	11
Figure 3.12	present results; solid lines denote the results by	
	Kuwahara et al. (2001).	70
Figure 5.13	A dimensionless velocity profile for $Pr = 1$ and	78
Figure 3.13	Re _D = 5×10^4 .	92
Figure 5.14	A dimensionless temperature profile for $Pr = 1$	82
Figure 3.14	and $Re_D = 5 \times 10^4$.	82
Figure 5.15	A nondimensional pressure field for $Re_D = 10^5$ and $\phi = 0.65$.	83
Figure 5.16	Isotherms for $Pr = 1$, $Re_D = 10^5$, and $\phi = 0.65$.	83
Figure 5.17	Turbulence kinetic energy for $Re_D = 10^5$ and $\phi = 0.65$.	83
	The effect of Re_D on h_i for $Pr = 1$ and $\phi = 0.65$.	84
Figure 5.18	The effect of Re_D on h_i for $Pr = 1$ and $\phi = 0.03$. The effect of porosity on h_i for $Pr = 1$.	
Figure 5.19 Figure 5.20		85
Figure 3.20	Comparison of the numerical results and the proposed	0.5
Eigura 5 21	correlation by Saito and de Lemos (2006).	85
Figure 5.21	Comparison of the numerical results and various	0.0
Eigene (1	correlations for $\phi = 0.65$.	86
Figure 6.1	The physical model and its coordinate system.	96
Figure 6.2	Porous media modeling, REV: (A) in-line array of square	
	rods; (B) triangular array of square rods; (C) unit cell for	0.0
	determining \mathbf{D}_{disp} .	98

List of Figures xxi

Figure 6.3	Neumann boundary conditions for mass fractions:	
	(A) longitudinal gradient; (B) transverse gradient.	99
Figure 6.4	Computational grids: (A) $\phi = 0.65$; (B) $\phi = 0.75$;	
	(C) $\phi = 0.90$.	100
Figure 6.5	Mass concentration fields for unit cells calculated with	
	longitudinal mass concentration gradients (laminar	
	regime— $Re_H = 1.0 \times 10$): (A) $\phi = 0.65$; (B) $\phi = 0.75$;	
	(C) $\phi = 0.90$.	101
Figure 6.6	Mass concentration fields for unit cells calculated with	
	longitudinal mass concentration gradients (turbulent	
	regime—high Reynolds model— $Re_H = 1.0 \times 10^6$):	
	(A) $\phi = 0.65$; (B) $\phi = 0.75$; (C) $\phi = 0.90$.	102
Figure 6.7	Mass concentration fields for unit cells calculated	
	with transverse mass concentration gradients (laminar	
	regime— $Re_H = 1.0 \times 10$): (A) $\phi = 0.65$; (B) $\phi = 0.75$;	
	(C) $\phi = 0.90$.	103
Figure 6.8	Mass concentration fields for unit cells calculated	
	with transverse mass concentration gradients (turbulent	
	regime—high Reynolds model— $Re_H = 1.0 \times 10^6$):	
	(A) $\phi = 0.65$; (B) $\phi = 0.75$; (C) $\phi = 0.90$.	104
Figure 6.9	Longitudinal mass dispersion coefficient for $\phi = 0.65$,	
	0.75, and 0.90; experimental data compiled by Han et al.	
	(1985), where more details on the experimental values can	
	be found.	107
Figure 6.10	The effect of porosity (ϕ) on the longitudinal dispersion	
	coefficient $(\mathbf{D}_{\text{disp}})_{XX}$.	108
Figure 6.11	Transverse mass dispersion coefficient for $\phi = 0.65, 0.75,$	
	and 0.90. Experimental values taken from Han et al. (1985),	
	where details on experimental data can be found.	108
Figure 6.12	The effect of porosity (ϕ) on the transversal dispersion	
	coefficient $(\mathbf{D}_{\text{disp}})_{\gamma\gamma}$.	109
Figure 6.13	The effect of the turbulence model on longitudinal mass	
	dispersion: (A) $\phi = 0.65$; (B) $\phi = 0.75$; (C) $\phi = 0.90$.	110
Figure 6.14	The effect of the turbulence model on transversal mass	
	dispersion: (A) $\phi = 0.65$; (B) $\phi = 0.75$; (C) $\phi = 0.90$.	111
Figure 7.1	The behavior of mixture density: (A) lighter mixture with	
	increasing $\langle \overline{T} \rangle^{i}$; (B) lighter mixture with increasing $\langle \overline{C} \rangle^{i}$;	
	(C) heavier mixture with increasing $(\overline{C})^i$.	116
Figure 7.2	Stability analysis of a layer of fluid subjected to gradients	
	of temperature and concentration. Unconditionally unstable	
	cases: hotter fluid (A) with less dense mixtures at the bottom	
	(B and C). Unconditionally stable cases: colder fluid	
Eigung 7.3	(D) with denser mixtures at the bottom (E and F).	120
Figure 7.3	Flows separated by a finite plate: (A) unconditionally	100
Figure 0.1	stable cases; (B) unconditionally unstable cases.	120
Figure 9.1	The representative elementary control volume for a	100
	moving porous bed.	135

xxii List of Figures

Figure 10.1	The trend of computational cost for a given	
	flow and algorithm.	144
Figure 10.2	The sparse matrix of coefficients for numerical fluid	
	dynamics problems.	144
Figure 10.3	Examples of computational grids.	146
Figure 10.4	Element transformation: (A) generalized coordinates	
	(ξ, η, γ) ; (B) Cartesian coordinates (x, y, z) .	147
Figure 10.5	Grid numbering.	149
Figure 10.6	Unstructured grids: (A) Voronoi diagram; (B) control-volume	
	finite element.	149
Figure 10.7	Three-dimensional structured grid for reservoir simulation.	150
Figure 10.8	A numerical treatment of petroleum reservoirs	
	(Maliska, 1995).	151
Figure 10.9	Grid layout for discretization methods: (A) finite volume;	
	(B) finite element.	152
Figure 10.10	Simplified schemes: (A) central differencing;	
	(B) upwind.	153
Figure 10.11	The effect of the interpolation scheme: (A) UPWIND—	
	numerical diffusion; (B) CDS—wiggles.	153
Figure 10.12	Advanced schemes: (A) second-order upwind;	
	(B) QUICK scheme.	154
Figure 10.13	The inclination of grid lines with respect to the	
	velocity vector.	154
Figure 10.14	(A) Geometry and boundary conditions; (B)	
	control-volume notation.	159
Figure 10.15	Different sweeping strategies: (A) SCGS, from node (i, j)	
	to $(i_{\text{max}}, j_{\text{max}})$ and back; (B) ASCGS, subsequent lines or	
	columns keep always physically connected cells in both	
	horizontal and vertical sweeping modes.	163
Figure 10.16	Grid independence studies: (A) vertical velocity	
	component; (B) Nusselt number.	164
Figure 10.17	Comparison of partially segregated and coupled results.	166
Figure 10.18	The effect of Ra on temperature and velocity fields—cavity	
	heated from below (HFB).	166
Figure 10.19	Temperature and velocity fields for a cavity heated	
	from left (VRT).	167
Figure 10.20	The effect of H/L on temperature for a vertical cavity	
	heated from left.	168
Figure 10.21	Streamlines for different aspect ratios for vertical cavities.	168
Figure 10.22	Isotherms for different cavity inclinations: HFB, $\alpha = 90^{\circ}$;	
	IFB, $\alpha = 45^{\circ}$; VRT, $\alpha = 0^{\circ}$; IFA, $\alpha = -85^{\circ}$; HFA,	
	$\alpha = -90^{\circ}$.	169
Figure 10.23	Vector plot for HFB case, $\alpha = 90^{\circ}$.	169
Figure 10.24	Residue history for HFB case: (A) relative and absolute mass	
	residues; (B) residue for energy equation.	170

List of Figures xxiii

Figure 10.25	Residue history for VRT case: (A) mass residue; (B) energy	
	equation residue.	171
Figure 10.26	Model combustor geometry and control-volume notation.	173
Figure 10.27	Residue history: (A) tangential velocity equation; (B) mass	
	residue for segregated and coupled methods.	181
Figure 10.28	A vertical cylindrical chamber.	183
Figure 10.29	Radial velocity U along the z-direction at $r = 0.5$ (A),	
	axial velocity along radius at $z = L/2 = R$ (B).	191
Figure 10.30	The effect of Re on the temperature field, $S = 1$, $Ra = 10^2$.	191
Figure 10.31	The effect of Ra on the temperature field, $Re = 2$, $S = 1$.	192
Figure 10.32	The effect of swirling strength S on temperature, $Ra = 10^4$,	102
FI 10.22	Re = 2.	193
Figure 10.33	The influence of Re on the convergence rate of the	
	T-equation.	194
Figure 10.34	The effect of Ra on R_T .	195
Figure 10.35	The effect of swirling strength S on R_T .	195
Figure 10.36	Mass residue history for segregated and coupled	
TI 10.05	approaches.	196
Figure 10.37	The influence of solution scheme on residue history of	
	energy equation.	197
Figure 10.38	The influence of solution scheme on convergence of	
	V-equation.	197
Figure 11.1	A model for channel flow with porous material: (A) without	• • • •
	the Forchheimer term; (B) with the Forchheimer term.	200
Figure 11.2	Notation for (A) control-volume discretization;	•
	(B) interface treatment.	203
Figure 11.3	The effect of grid size on the velocity field: (A) without	201
	the Forchheimer term; (B) with the Forchheimer term.	206
Figure 11.4	Comparison between analytical and numerical	
	solutions for different values of permeability, K: (A)	
	without the Forchheimer term; (B) with the Forchheimer	200
	term.	208
Figure 11.5	Comparison between analytical and numerical solutions	
	for different porosities, ϕ : (A) without the Forchheimer term;	200
F:	(B) with the Forchheimer term.	209
Figure 11.6	Comparison between analytical and numerical solutions for	
	different values of β : (A) without the Forchheimer term;	210
F: 11.5	(B) with the Forchheimer term.	210
Figure 11.7	The effect of mesh size on a numerical solution.	214
Figure 11.8	The effect of Reynolds number, Re_H , on macroscopic field:	
E' 110	(A) mean velocity; (B) turbulent kinetic energy.	215
Figure 11.9	The effect of permeability, K, on macroscopic field:	211
E: 11 10	(A) mean velocity; (B) turbulent kinetic energy.	216
Figure 11.10	The effect of porosity on macroscopic field: (A) mean	21-
	velocity; (B) turbulent kinetic energy.	217

xxiv List of Figures

Figure 11.11	The effect of parameter, β , on hydrodynamic field: (A) mean velocity; (B) turbulent field.	219
Figure 11.12	Calculations using Eq. (11.40) (lines) compared with	217
rigure 11.12	simulations with Eq. (11.43) (symbols) and $\beta = 0$: (A) mean	
	field; (B) turbulent field.	223
Figure 11.13	The effect of jump conditions on mean and turbulent fields:	
riguio rinio	(A) mean velocity u ; (B) nondimensional turbulent kinetic	
	energy.	225
Figure 11.14	The effect of Reynolds number Re_H on the macroscopic	
1.80.0	field. β < 0: (A) mean velocity; (B) turbulent kinetic energy.	
	$\beta > 0$: (C) mean velocity; (D) turbulent kinetic energy.	226
Figure 11.15	The effect of permeability, <i>K</i> , on the macroscopic field.	220
	β < 0: (A) mean velocity; (B) turbulent kinetic energy.	
	$\beta > 0$: (C) mean velocity; (D) turbulent kinetic energy.	227
Figure 11.16	The effect of porosity, ϕ , on the macroscopic field. β < 0:	
8	(A) mean velocity; (B) turbulent kinetic energy. $\beta > 0$:	
	(C) mean velocity; (D) turbulent kinetic energy.	228
Figure 11.17	The problem under consideration: (A) geometry; (B) channel	
	cell; (C) section of computational grid of length 2L.	230
Figure 11.18	Developing Nu and f for a channel with solid baffles,	
8	$h/H = 0.5$, $\lambda = 0.4$: (A) $Re = 100$; (B) $Re = 300$;	
	(C) $Re = 500$.	234
Figure 11.19	Developing Nu and f for a channel with porous fins,	
C	$h/H = 0.5$, $K = 1 \times 10^{-9}$ m ² , $\phi = 0.4$, $\lambda = 0.4$: (A) $Re = 100$;	
	(B) $Re = 300$; (C) $Re = 500$.	235
Figure 11.20	Streamlines a pattern as a function of Re for $h/H = 0.5$:	
	(A) solid baffles (Kelkar and Patankar, 1987); (B) present	
	work, solid baffles; (C) present work, porous baffles,	
	$K = 1 \times 10^{-9} \mathrm{m}^2, \phi = 0.4.$	237
Figure 11.21	Streamlines a pattern as a function of h/H , $Re = 300$:	
	(A) solid baffles; (B) porous baffles, $K = 1 \times 10^{-9} \text{ m}^2$,	
	$\phi = 0.4$.	238
Figure 11.22	Streamlines a pattern as a function of K for $h/H = 0.5$	
	and $\phi = 0.9$: (A) $K = 1 \times 10^{-9} \text{ m}^2$; (B) $K = 1 \times 10^{-8} \text{ m}^2$;	
	(C) $K = 1 \times 10^{-7} \text{ m}^2$.	239
Figure 11.23	Streamlines as a function of ϕ , $Re = 500$, $h/H = 0.5$:	
	(A) $K = 1 \times 10^{-9} \text{ m}^2$, (B) $K = 1 \times 10^{-7} \text{ m}^2$; (C)	
	$K = 1 \times 10^{-5} \text{ m}^2$.	240
Figure 11.24	Friction factor for a channel as a function of Re , $h/H = 0.5$:	
	(A) solid baffles; (B) porous baffles.	241
Figure 11.25	Friction factor for a channel with baffles: (A) effect of ϕ ,	
	$h/H = 0.5$; (B) effect of h/H , $K = 1 \times 10^{-9}$ m ² , and $\phi = 0.4$.	242
Figure 11.26	The Nusselt number for a channel as a function of Re,	
	$h/H = 0.5$: (A) solid baffles; (B) effect of K and ϕ , $\lambda = 0.4$,	
	$Pr = 0.7$; (C) effect of λ and ϕ , $K = 1 \times 10^{-9}$ m ² , and	
	Pr = 0.7.	243